

Exact relations between magnetoresistivity tensor components of conducting composites with a columnar microstructure

Yakov M. Strelniker and David J. Bergman

School of Physics and Astronomy, Raymond and Beverly Sackler Faculty of Exact Sciences, Tel Aviv University, Tel Aviv 69978, Israel

(Received 3 August 1999)

A recently discovered duality transformation for a three-dimensional columnar medium (i.e., a medium that is uniform along some fixed direction, called the columnar axis) is applied to a two-constituent composite medium. This leads to a generalization of Keller's theorem: Exact relations are found between in-plane components (i.e., components that are perpendicular to the columnar axis) of the bulk effective resistivity or conductivity tensor of the columnar composite medium and similar quantities of a dual problem. These are used to find exact relations between in-plane bulk effective magnetoresistivity and magnetoconductivity components of a conductor/insulator mixture and those of a normal conductor/perfect conductor mixture *with the same microstructure*. The exact relations are applied to and tested on a number of available results on in-plane magnetoresistance in columnar composites, including an effective medium approximation, numerical computations on periodic microstructures, and closed form expressions for the asymptotic behavior at strong magnetic fields in periodic microstructures.

I. INTRODUCTION

The macroscopic or bulk effective moduli of a composite medium depend on its detailed microstructure, and can usually be calculated only approximately. Notwithstanding this generic feature, there exist some exact, microstructure-independent results for such moduli in the case of two-dimensional (2D) composites. These go back to a pioneering paper by Landauer and his associates, where it was shown that the bulk effective Hall resistivity of a thin conducting film with a collection of punched holes is independent of the number or shapes or locations of the holes.¹ In another pioneering paper, Keller showed that, in a 2D rectangular periodic array of inclusions, the bulk effective principal conductivities of the ‘‘phase exchanged composites’’ $\sigma_{yy}^{(e)}(\sigma_1, \sigma_2)$ and $\sigma_{zz}^{(e)}(\sigma_2, \sigma_1)$ are related in the following way:²

$$\sigma_{yy}^{(e)}(\sigma_1, \sigma_2)\sigma_{zz}^{(e)}(\sigma_2, \sigma_1) = \sigma_1\sigma_2. \quad (1.1)$$

Here the two composites have the *same microstructure* but the two constituents, with scalar conductivities σ_1 , σ_2 , have exchanged their spatial locations. This theorem became a powerful tool in many studies of electrical transport problems. Thus it is no surprise that attempts were made to extend it in various ways: Dykhne³ discovered the duality transformation for classical transport problems in 2D, which greatly facilitates the derivation of Eq. (1.1), and enabled Mendelson to generalize it to the case where the microstructure is arbitrary,⁴ and also to the case where the constituent conductivities are arbitrary, nonsymmetric, 2×2 tensors.⁵ Schulgasser⁶ derived an exact microstructure-independent expression for the conductivity of an isotropic polycrystalline film made using a single anisotropic constituent, but with a random distribution of crystallite orientations. Separate progress was made by Shklovskii,⁷ who exploited the classical duality transformation in order to derive an exact expression for the bulk effective weak-field Hall conductivity in terms of the bulk effective zero field Ohmic conduc-

tivity for a 2D, isotropic, two-constituent composite conductor. Stroud and Bergman⁸ used that transformation to show that, like the Hall resistivity, the relative Ohmic magnetoresistivity of a thin metal film with holes, and subject to a perpendicular magnetic field, is equal to that of the uniform metal film, and is independent of any details of the hole configuration. That result was extended to arbitrary 2D composites by Milton,⁹ and was tested on numerical computations by Christiansson.¹⁰ Those results have been applied to a discussion of the fractional quantum Hall effect.^{11,12} The duality transformation has also been applied to nonlinear electrical transport problems—see Ref. 13, where previous works are also cited.

However, all of these developments were confined to the case of a strictly 2D composite, or at most to a columnar system with a magnetic field along the columnar axis, where the electric field and flux are 2D. In spite of the thirty five years elapsed since Keller's pioneering work,² all attempts to extend those results to more general types of three-dimensional (3D) systems were unsuccessful, except for some inequalities found by Schulgasser.⁶ In fact, that article provides a proof of the ‘‘nonexistence of a Keller-type theorem in three dimensions.’’

In this article we present a Keller-type theorem for 3D systems with a columnar microstructure, i.e., for macroscopically inhomogeneous media that are uniform in one fixed direction. Such systems can exhibit nontrivial 3D electrical transport behavior when the conductivity tensors are nonscalar. More specifically, we consider the case of a two-constituent composite with a columnar microstructure, where both components are isotropic conductors but a magnetic field is present that is perpendicular to the columnar axis, i.e., an ‘‘in-plane’’ magnetic field. In such a system, the presence of a Hall effect ensures that the conductivity tensors are not only nonscalar, but also nonsymmetric, and that nontrivial electrical transport occurs in all directions. We note that, although such microstructures are special, i.e., they are not generic 3D microstructures, they are nevertheless very

common and very important, especially in fiber reinforced composites and also in various types of thin films. In particular, a thin film with a periodic columnar microstructure, such as a periodic array of perpendicular cylindrical etched holes, is much easier to fabricate than any 3D periodic array. Some exact results were recently obtained for columnar components of the bulk effective resistivity tensor $\hat{\rho}_e$ in such systems.¹⁴ Also recently, a duality transformation was discovered that can always be applied to columnar systems, even when the fields and fluxes are truly 3D.^{15,16} Closed form asymptotic (strong magnetic field) expressions were obtained for the bulk effective in-plane magnetoresistivity of such systems, where the columnar microstructure is periodic and the magnetic field lies along a low order lattice axis of the 2D periodic array. Some of those expressions were already found empirically to exhibit a surprisingly simple connection between the case of a conductor/perfect insulator mixture and a normal conductor/perfect conductor mixture.¹⁵ Here we will derive some simple, general, exact relations, which are generalizations of Eq. (1.1) and of the relation discovered empirically in Ref. 15. These lead to simple connections, that must always hold between in-plane magnetoresistivity components of a conductor/perfect insulator mixture and those of a normal conductor/perfect conductor mixture with the *same columnar microstructure* but *irrespective of any other microstructural details*, and for *arbitrary values of the in-plane magnetic field*.

The remainder of this article is organized as follows. In Sec. II we summarize the theory needed in order to discuss a composite conductor with a columnar microstructure,¹⁷ subject to a uniform applied magnetic field. This includes the recently discovered classical duality transformation for 3D systems with such a microstructure.^{15,16} In Sec. III we prove some exact relations between the conductivity components of the original problem and those of a dual problem. In Sec. IV we apply these results in order to derive exact, simple relations between the in-plane magnetoresistivity or magnetoconductivity components of a conductor/perfect insulator mixture and those of a normal conductor/perfect conductor mixture with the *same columnar microstructure*. In Sec. V we illustrate the consequences and power of these relations by testing them on a recently developed effective-medium approximation,¹⁴ on closed-form asymptotic expressions for magnetoresistivity in periodic columnar composites,^{15,16} and also on numerical computations of magnetoresistivity in such composites. Section VI provides a summary of the main results.

II. THEORY

A. Basic concepts

The electrical transport on the microscale is assumed to be describable in terms of a local curl-free electric field $\mathbf{E}(\mathbf{r}) \equiv \nabla \phi(\mathbf{r})$ and a local divergence-free current density or flux $\mathbf{J}(\mathbf{r})$, which are related to each other linearly by means of a local resistivity tensor $\hat{\rho}(\mathbf{r})$ or a local conductivity tensor $\hat{\sigma}(\mathbf{r}) = 1/\hat{\rho}(\mathbf{r})$

$$\mathbf{J}(\mathbf{r}) = \hat{\sigma}(\mathbf{r}) \cdot \mathbf{E}(\mathbf{r}). \quad (2.1)$$

These fields are found by solving the usual equation

$$\nabla \cdot \hat{\sigma} \cdot \nabla \phi = 0, \quad (2.2)$$

with appropriate boundary conditions on the electrical potential $\phi(\mathbf{r})$.

We can express $\hat{\sigma}(\mathbf{r})$ in terms of the constituent conductivity tensors $\hat{\sigma}_i$ and the characteristic (or indicator) functions $\theta_i(\mathbf{r})$ [$\theta_i(\mathbf{r}) = 1$ if $\hat{\sigma}(\mathbf{r}) = \hat{\sigma}_i$, otherwise $\theta_i(\mathbf{r}) = 0$]. In the case of a two-constituent composite medium we can thus write

$$\hat{\sigma}(\mathbf{r}) = \hat{\sigma}_1 \theta_1(\mathbf{r}) + \hat{\sigma}_2 \theta_2(\mathbf{r}) = \hat{\sigma}_2 - \delta \hat{\sigma} \theta_1(\mathbf{r}), \quad (2.3)$$

$$\delta \hat{\sigma} \equiv \hat{\sigma}_2 - \hat{\sigma}_1. \quad (2.4)$$

Using this, the differential equation (2.2) can be written as

$$\nabla \cdot \hat{\sigma}_2 \cdot \nabla \phi = \nabla \cdot \delta \hat{\sigma} \theta_1 \cdot \nabla \phi. \quad (2.5)$$

The bulk effective conductivity tensor of the composite $\hat{\sigma}^{(e)}$ is defined as providing the linear relationship between the volume averages of the electric field $\nabla \phi(\mathbf{r})$ and the current density $\mathbf{J}(\mathbf{r}) \equiv \hat{\sigma}(\mathbf{r}) \cdot \nabla \phi(\mathbf{r})$

$$\langle \mathbf{J} \rangle \equiv \hat{\sigma}^{(e)} \cdot \langle \nabla \phi(\mathbf{r}) \rangle, \quad (2.6)$$

where $\langle \rangle$ denotes a volume average over the entire system. Equivalently, the bulk effective resistivity tensor $\hat{\rho}^{(e)} = 1/\hat{\sigma}^{(e)}$ can be obtained from

$$\hat{\rho}^{(e)} \cdot \langle \mathbf{J} \rangle \equiv \langle \mathbf{E} \rangle. \quad (2.7)$$

The bulk effective tensors $\hat{\sigma}^{(e)}$, $\hat{\rho}^{(e)}$ characterize the macroscopic electrical response of the system, i.e., its transport behavior on length scales much larger than the typical microstructure or heterogeneity length scales, when we are interested only in some coarse-grained volume averaged values of \mathbf{E} and \mathbf{J} .

The final result for $\hat{\sigma}^{(e)}$ will be independent of the precise way in which $\phi(\mathbf{r})$ is produced, provided that the composite microstructure, as well as the boundary conditions that determine $\phi(\mathbf{r})$, are macroscopically homogeneous. We are therefore free to choose the most convenient among a rather general class of possible boundary conditions when setting up a scheme for calculating $\phi(\mathbf{r})$. We choose a scheme where the composite medium occupies the entire volume in between the infinitely conducting plates of a parallel plate capacitor. The plates are taken to be infinitely large, and the distance between them is taken to be finite but large compared to any scale of inhomogeneity of the system. Keeping the medium and the magnetic field fixed, we can choose the orientation of the plates to be perpendicular to any of the coordinate axes. We denote by $\phi^{(\alpha)}(\mathbf{r})$ the local potential field which results when the plates are perpendicular to the r_α axis, and a potential difference equal to their distance apart L is applied between them. The volume averaged electric field is then $\langle \nabla \phi^{(\alpha)} \rangle = \nabla r_\alpha = \mathbf{e}_\alpha$, i.e., a unit vector in the r_α direction.

Using Eqs. (2.3) and (2.6) we can write the following expression for $\hat{\sigma}^{(e)}$:

$$\hat{\sigma}^{(e)} \cdot \langle \nabla \phi^{(\alpha)} \rangle = \hat{\sigma}_2 \cdot \langle \nabla \phi^{(\alpha)} \rangle - \delta \hat{\sigma} \cdot \langle \theta_1 \nabla \phi^{(\alpha)} \rangle. \quad (2.8)$$

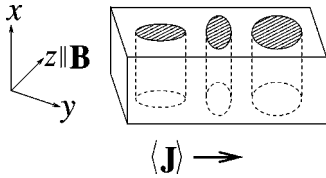


FIG. 1. Composite conductor with columnar microstructure shaped as a wire or thin film, with the film plane, magnetic field $\mathbf{B} \parallel z$, and volume averaged current density $\langle \mathbf{J} \rangle$ all perpendicular to the columnar axis x .

This can be further processed, by recalling that $\langle \nabla \phi^{(\alpha)} \rangle = \mathbf{e}_\alpha$, to yield

$$\sigma_{\alpha\beta}^{(e)} = \sigma_{2\alpha\beta} - \sum_{\gamma} \delta\sigma_{\alpha\gamma} \cdot \langle \theta_1 \nabla_{\gamma} \phi^{(\beta)} \rangle. \quad (2.9)$$

Further considerations simplify if we note that some of the components of the resistivity and conductivity tensors vanish, while others are simply related to each other, when the coordinate axes are chosen to lie along the principal axes of the system, and the magnetic field \mathbf{B} lies along one of them, always taken to be the z axis. In this case we can write

$$\hat{\rho} = \begin{pmatrix} \rho_{xx} & \rho_{xy} & 0 \\ \rho_{yx} & \rho_{yy} & 0 \\ 0 & 0 & \rho_{zz} \end{pmatrix}, \quad \hat{\sigma} = \begin{pmatrix} \sigma_{xx} & \sigma_{xy} & 0 \\ \sigma_{yx} & \sigma_{yy} & 0 \\ 0 & 0 & \sigma_{zz} \end{pmatrix}, \quad (2.10)$$

where $\rho_{xy} = -\rho_{yx}$ and $\sigma_{xy} = -\sigma_{yx}$. For a free-electron Drude metal, these matrices take the form

$$\hat{\rho} = \rho_0 \begin{pmatrix} 1 & -H & 0 \\ H & 1 & 0 \\ 0 & 0 & 1 \end{pmatrix}, \quad \hat{\sigma} = \frac{1}{\rho_0} \begin{pmatrix} \frac{1}{1+H^2} & \frac{H}{1+H^2} & 0 \\ -H & 1 & 0 \\ \frac{1}{1+H^2} & \frac{1}{1+H^2} & 0 \\ 0 & 0 & 1 \end{pmatrix}, \quad (2.11)$$

where ρ_0 is the Ohmic resistivity, which is independent of \mathbf{B} , and $H = \omega_c \tau = \mu |\mathbf{B}|$ denotes the Hall-to-Ohmic resistivity ratio ($\omega_c = e |\mathbf{B}| / mc$ is the cyclotron frequency and μ is the Hall mobility—both have the same sign as the charge e of the charge carriers; τ is the transport relaxation time).

B. Columnar microstructures

Consider a heterogeneous medium, characterized by a local resistivity tensor that depends only upon y and z . This is a 3D medium with 2D heterogeneity, with the x axis as columnar symmetry axis—see Fig. 1. It is easy to see that all components of $\mathbf{J}(\mathbf{r})$ and $\mathbf{E}(\mathbf{r})$ must be independent of x , if the boundary conditions would result in uniform values of $\mathbf{J}(\mathbf{r})$ and $\mathbf{E}(\mathbf{r})$ in a homogeneous medium

$$\mathbf{E}(\mathbf{r}) = \mathbf{E}(y, z); \quad \mathbf{J}(\mathbf{r}) = \mathbf{J}(y, z). \quad (2.12)$$

From the local curl-free condition $\nabla \times \mathbf{E} = 0$, it then follows that¹⁷

$$E_x = \text{const everywhere}. \quad (2.13)$$

The only exception to these rules occurs near the boundaries. Those surface effects can be neglected if the sample size l along the columnar axis and the heterogeneity length scale a satisfy $a/l \ll \max(1, |\mu B_{\perp}|)$, where B_{\perp} is the component of \mathbf{B} perpendicular to x —see Ref. 18. We note that, in spite of the 2D heterogeneity, the transport processes will have an essentially 3D character. I.e., the local flux $\mathbf{J}(\mathbf{r})$ will usually have a nonzero component along the columnar symmetry axis x whenever $B_{\perp} \neq 0$, even if the macroscopic or volume averaged flux $\langle \mathbf{J} \rangle$ is also perpendicular to x .

We now derive exact expressions for the bulk effective resistivity components $\rho_{xx}^{(e)}$ and $\rho_{xy}^{(e)}$ of a columnar microstructure made of a percolating conducting host and nonpercolating inclusions that are either perfect insulators or perfect conductors. Those expressions are special cases of the more general expressions obtained in Ref. 14.

We start from the relation

$$E_x = \rho_{xx} J_x + \rho_{xy} J_y, \quad (2.14)$$

where each of the quantities on the right-hand side (rhs) usually depends on \mathbf{r} , but when taken together they must lead to a position independent value for E_x . In the case of a conductor/insulator mixture, \mathbf{J} vanishes inside the insulating constituent, therefore we can average this equation over the conducting subvolume to get

$$E_x = \frac{1}{p_M} (\rho_{xx}^{(M)} \langle J_x \rangle + \rho_{xy}^{(M)} \langle J_y \rangle). \quad (2.15)$$

Here $\rho_{xx}^{(M)}, \rho_{xy}^{(M)}$ are resistivity components of the conducting constituent, and the factor p_M , which denotes the volume fraction of that constituent, appears because $\langle J_x \rangle, \langle J_y \rangle$ denote averages over the *entire system volume*. The last equation permits us to read off the following results:

$$\rho_{xx \text{ ins}}^{(e)} = \frac{\rho_{xx}^{(M)}}{p_M}, \quad \rho_{xy \text{ ins}}^{(e)} = \frac{\rho_{xy}^{(M)}}{p_M}, \quad \rho_{xz \text{ ins}}^{(e)} = 0, \quad (2.16)$$

where the subscript ‘ins’ obviously identifies the result as pertaining to a conductor/insulator mixture. The fact that $\rho_{yx}^{(e)} = -\rho_{xy}^{(e)}$ and $\rho_{zx}^{(e)} = -\rho_{xz}^{(e)}$ follows from the duality symmetry, as shown in Eqs. (2.25) in the following subsection. Thus, all the resistivity components that lie in the first row and column of $\hat{\rho}_{\text{ins}}^{(e)}$ are completely determined and depend only on the conducting constituent volume fraction p_M .

In the case of a normal conductor/perfect conductor mixture, \mathbf{E} vanishes inside the perfectly conducting inclusions, therefore E_x , which is uniform, vanishes everywhere. At the same time, $\langle J_x \rangle, \langle J_y \rangle$, and $\langle J_z \rangle$ are usually nonzero, therefore

$$\rho_{xx \text{ sup}}^{(e)} = \rho_{xy \text{ sup}}^{(e)} = \rho_{yx \text{ sup}}^{(e)} = \rho_{xz \text{ sup}}^{(e)} = \rho_{zx \text{ sup}}^{(e)} = 0, \quad (2.17)$$

where the subscript ‘sup’ identifies the result as pertaining to a normal conductor/perfect conductor mixture, and where we again used Eqs. (2.25). Again, all the elements in the first row and column of $\hat{\rho}_{\text{sup}}^{(e)}$ are completely determined—they all vanish.

C. Duality in a 3D system with columnar symmetry

The classical duality symmetry²⁻⁴ is based upon the fact that a 2D curl-free vector field becomes divergence-free when it is rotated by 90° in the plane, while a 2D divergence-free vector field becomes curl-free when it is similarly rotated. 3D vector fields usually lack those properties. Because \mathbf{B} does not lie along the columnar axis, therefore the electrical transport always has a 3D character: Even if the volume averaged current density $\langle \mathbf{J} \rangle$ lies in the y, z plane, the local Hall effect, in conjunction with the heterogeneous microstructure, will usually induce local fields and currents in all directions. However, in Refs. 15 and 16 it was shown that, for the special case of electrical conduction in a 3D system with a 2D heterogeneity, there exists a nontrivial duality transformation. A brief description follows.

In a columnar system, where \mathbf{E} and \mathbf{J} are 3D fields, we perform a 90° rotation only of the y and z components of those fields, i.e., the in-plane components, leaving the columnar or x components intact. We then define the dual electric field \mathbf{E}_D and dual current density \mathbf{J}_D as follows:

$$\mathbf{E}_D \equiv (E_x, -\rho_0 J_z, \rho_0 J_y), \quad \mathbf{J}_D \equiv (J_x, -E_z/\rho_0, E_y/\rho_0). \quad (2.18)$$

Here a constant (i.e., position independent) resistivity ρ_0 was introduced in order to make the physical dimensions of the different components of \mathbf{E}_D and \mathbf{J}_D consistent. For simplicity we will usually choose this constant to be the same as the Ohmic resistivity of the host constituent, which we take to be a simple free-electron conductor. It is easy to see that $\nabla \cdot \mathbf{J}_D = \nabla \times \mathbf{E}_D = 0$.

From these definitions, it is easy to write a linear relation between \mathbf{J}_D and \mathbf{E}_D :

$$\mathbf{J}_D = \hat{\sigma}_D \cdot \mathbf{E}_D, \quad \mathbf{E}_D = \hat{\rho}_D \cdot \mathbf{J}_D, \quad (2.19)$$

where

$$\rho_0 \hat{\sigma}_D = \begin{pmatrix} \frac{\rho_0}{\rho_{xx}} & -\frac{\rho_{xz}}{\rho_{xx}} & \frac{\rho_{xy}}{\rho_{xx}} \\ \frac{\rho_{zx}}{\rho_{xx}} & \frac{\rho_{zz}}{\rho_0} - \frac{\rho_{xz}\rho_{zx}}{\rho_0\rho_{xx}} & -\frac{\rho_{zy}}{\rho_0} + \frac{\rho_{xy}\rho_{zx}}{\rho_0\rho_{xx}} \\ -\frac{\rho_{yx}}{\rho_{xx}} & -\frac{\rho_{yz}}{\rho_0} + \frac{\rho_{xz}\rho_{yx}}{\rho_0\rho_{xx}} & \frac{\rho_{yy}}{\rho_0} - \frac{\rho_{xy}\rho_{yx}}{\rho_0\rho_{xx}} \end{pmatrix}. \quad (2.20)$$

Note that this holds for the local dual conductivity tensor components describing any kind of constituent of the composite medium, as well as for the bulk effective tensor components which characterize the macroscopic overall response of the composite medium.

When $\hat{\rho}$ and $\hat{\sigma}$ have the forms shown in Eqs. (2.10), then this generic form of $\rho_0 \hat{\sigma}_D$ can be simplified to

$$\rho_0 \hat{\sigma}_D = \begin{pmatrix} \frac{\rho_0}{\rho_{xx}} & 0 & -\frac{\sigma_{xy}}{\sigma_{yy}} \\ 0 & \frac{1}{\rho_0 \sigma_{zz}} & 0 \\ \frac{\sigma_{yx}}{\sigma_{yy}} & 0 & \frac{1}{\rho_0 \sigma_{yy}} \end{pmatrix}. \quad (2.21)$$

A particular case of this occurs when the host is a free-electron metal, and the system is subject to a uniform magnetic field $\mathbf{B} \parallel z$ [see Eq. (2.11)]. In that case, the dual conductivity tensor has the form

$$\hat{\sigma}_{D \text{ free el}} = \frac{1}{\rho_0} \begin{pmatrix} 1 & 0 & -H \\ 0 & 1 & 0 \\ -H & 0 & 1+H^2 \end{pmatrix}. \quad (2.22)$$

The fact that this $\hat{\sigma}_D$ is symmetric, even though $\hat{\rho}$ and $\hat{\sigma}$ of Eq. (2.11) have an antisymmetric Hall component, is both remarkable and useful: Conductivity problems with a symmetric conductivity tensor are easier to consider intuitively, and they also satisfy a simple variational principle—see Refs. 15 and 19.

The dual conductivity tensor of the inclusions can be determined in a similar fashion. If the inclusions are *perfectly insulating* $\hat{\rho}_{\text{ins}} = \infty \times \hat{I}$, (\hat{I} is the unit tensor) then their dual conductivity tensor is

$$\hat{\sigma}_{D \text{ ins}} = \begin{pmatrix} 0 & 0 & 0 \\ 0 & \infty & 0 \\ 0 & 0 & \infty \end{pmatrix}. \quad (2.23)$$

In the opposite case, when the inclusions are *perfect conductors*, then the dual conductivity tensor is

$$\hat{\sigma}_{D \text{ sup}} = \begin{pmatrix} \infty & 0 & 0 \\ 0 & 0 & 0 \\ 0 & 0 & 0 \end{pmatrix}. \quad (2.24)$$

Note, also, that the electric field \mathbf{E} must vanish inside such inclusions, therefore $E_x \equiv 0$ everywhere.

Since the dual conductivity tensors of Eqs. (2.22)–(2.24) are all symmetric, therefore any composite made of those constituents will have a bulk effective dual conductivity tensor $\hat{\sigma}_D^{(e)}$ which is also symmetric. From Eq. (2.20), that means we must have

$$\rho_{xz}^{(e)} = -\rho_{zx}^{(e)}, \quad \rho_{xy}^{(e)} = -\rho_{yx}^{(e)}, \quad \rho_{yz}^{(e)} = \rho_{zy}^{(e)}. \quad (2.25)$$

III. EXACT RELATION BETWEEN THE BULK EFFECTIVE CONDUCTIVITIES OF THE ORIGINAL PROBLEM AND A DUAL PROBLEM

The partial differential equation (2.5) can be applied to the original physical problem (using the potential ϕ , and conductivities $\hat{\sigma}$, $\delta\hat{\sigma}$) as well as to the dual problem (using the potential ϕ_D , and conductivities $\hat{\sigma}_D$, $\delta\hat{\sigma}_D$). Taking into account that $\hat{\sigma}$ has the form (2.10), while $\hat{\sigma}_D$ has the form

(2.21), and using the fact that \mathbf{E} , \mathbf{E}_D , and θ_1 are independent of x , and that $E_x \equiv E_{D,x} \equiv \text{const}$, we get the following equations for ϕ and ϕ_D :

$$\begin{aligned} \sigma_{2yy} \frac{\partial^2 \phi}{\partial y^2} + \sigma_{2zz} \frac{\partial^2 \phi}{\partial z^2} &= \delta\sigma_{yy} \frac{\partial}{\partial y} \left(\theta_1 \frac{\partial \phi}{\partial y} \right) + \delta\sigma_{zz} \frac{\partial}{\partial z} \left(\theta_1 \frac{\partial \phi}{\partial z} \right) \\ &+ \delta\sigma_{yx} \frac{\partial}{\partial y} \left(\theta_1 \frac{\partial \phi}{\partial x} \right), \end{aligned} \quad (3.1)$$

$$\begin{aligned} \sigma_{D2yy} \frac{\partial^2 \phi_D}{\partial y^2} + \sigma_{D2zz} \frac{\partial^2 \phi_D}{\partial z^2} \\ = \delta\sigma_{Dyy} \frac{\partial}{\partial y} \left(\theta_1 \frac{\partial \phi_D}{\partial y} \right) + \delta\sigma_{Dzz} \frac{\partial}{\partial z} \left(\theta_1 \frac{\partial \phi_D}{\partial z} \right) \\ + \delta\sigma_{Dzx} \frac{\partial}{\partial z} \left(\theta_1 \frac{\partial \phi_D}{\partial x} \right). \end{aligned} \quad (3.2)$$

We now define new potential fields φ , φ_D by adding terms to ϕ , ϕ_D that are linear in y , z , respectively:

$$\phi \equiv \varphi - \frac{\delta\sigma_{yx}}{\delta\sigma_{yy}} \left(\frac{\partial \phi}{\partial x} \right) y, \quad (3.3)$$

$$\phi_D \equiv \varphi_D - \frac{\delta\sigma_{Dzx}}{\delta\sigma_{Dzz}} \left(\frac{\partial \phi_D}{\partial x} \right) z. \quad (3.4)$$

The new fields satisfy somewhat simpler differential equations, namely

$$\sigma_{2yy} \frac{\partial^2 \varphi}{\partial y^2} + \sigma_{2zz} \frac{\partial^2 \varphi}{\partial z^2} = \delta\sigma_{yy} \frac{\partial}{\partial y} \left(\theta_1 \frac{\partial \varphi}{\partial y} \right) + \delta\sigma_{zz} \frac{\partial}{\partial z} \left(\theta_1 \frac{\partial \varphi}{\partial z} \right), \quad (3.5)$$

$$\begin{aligned} \sigma_{D2yy} \frac{\partial^2 \varphi_D}{\partial y^2} + \sigma_{D2zz} \frac{\partial^2 \varphi_D}{\partial z^2} &= \delta\sigma_{Dyy} \frac{\partial}{\partial y} \left(\theta_1 \frac{\partial \varphi_D}{\partial y} \right) \\ &+ \delta\sigma_{Dzz} \frac{\partial}{\partial z} \left(\theta_1 \frac{\partial \varphi_D}{\partial z} \right). \end{aligned} \quad (3.6)$$

From Eq. (2.9) we get the following expressions for the in-plane components of $\hat{\sigma}^{(e)}$ and $\hat{\sigma}_D^{(e)}$ in terms of the renormalized potentials φ , φ_D :

$$\sigma_{yy}^{(e)} = \sigma_{2yy} - \delta\sigma_{yy} \left\langle \theta_1 \frac{\partial \varphi^{(y)}}{\partial y} \right\rangle, \quad (3.7)$$

$$\sigma_{zz}^{(e)} = \sigma_{2zz} - \delta\sigma_{zz} \left\langle \theta_1 \frac{\partial \varphi^{(z)}}{\partial z} \right\rangle, \quad (3.8)$$

$$\sigma_{yz}^{(e)} = -\delta\sigma_{yy} \left\langle \theta_1 \frac{\partial \varphi^{(z)}}{\partial y} \right\rangle, \quad (3.9)$$

$$\sigma_{zy}^{(e)} = -\delta\sigma_{zz} \left\langle \theta_1 \frac{\partial \varphi^{(y)}}{\partial z} \right\rangle, \quad (3.10)$$

$$\sigma_{Dyy}^{(e)} = \sigma_{D2yy} - \delta\sigma_{Dyy} \left\langle \theta_1 \frac{\partial \varphi_D^{(y)}}{\partial y} \right\rangle, \quad (3.11)$$

$$\sigma_{Dzz}^{(e)} = \sigma_{D2zz} - \delta\sigma_{Dzz} \left\langle \theta_1 \frac{\partial \varphi_D^{(z)}}{\partial z} \right\rangle, \quad (3.12)$$

$$\sigma_{Dyz}^{(e)} = -\delta\sigma_{Dyy} \left\langle \theta_1 \frac{\partial \varphi_D^{(z)}}{\partial y} \right\rangle, \quad (3.13)$$

$$\sigma_{Dzy}^{(e)} = -\delta\sigma_{Dzz} \left\langle \theta_1 \frac{\partial \varphi_D^{(y)}}{\partial z} \right\rangle. \quad (3.14)$$

We note that the transformed potentials $\varphi^{(y)}$, $\varphi^{(z)}$, $\varphi_D^{(y)}$, $\varphi_D^{(z)}$ are the same as $\phi^{(y)}$, $\phi^{(z)}$, $\phi_D^{(y)}$, $\phi_D^{(z)}$, due to the fact that these potentials are all independent of x . Moreover, these potentials, as well as the bulk effective in-plane conductivity components $\sigma_{yy}^{(e)}$, $\sigma_{zz}^{(e)}$, $\sigma_{Dyy}^{(e)}$, $\sigma_{Dzz}^{(e)}$, depend only upon the in-plane conductivity components of the two constituents σ_{iyy} , σ_{izz} , $i=1,2$. The other conductivity components of the two constituents σ_{ixx} , σ_{ixy} , σ_{iyx} , $i=1,2$ have no effect on the values of $\sigma_{yy}^{(e)}$, $\sigma_{zz}^{(e)}$, $\sigma_{Dyy}^{(e)}$, $\sigma_{Dzz}^{(e)}$. This observation will turn out to have important consequences.

In order to make Eqs. (3.5) and (3.6) as similar as possible to each other, we would like to make the constant coefficients in the two equations proportional to each other. Noting that [see Eq. (2.21)]

$$\frac{\sigma_{2yy}}{\sigma_{D2yy}} = \rho_0^2 \sigma_{2yy} \sigma_{2zz}, \quad (3.15)$$

$$\frac{\sigma_{2zz}}{\sigma_{D2zz}} = \rho_0^2 \sigma_{2yy} \sigma_{2zz}, \quad (3.16)$$

$$\frac{\delta\sigma_{yy}}{\delta\sigma_{Dyy}} = \frac{\sigma_{2yy} - \sigma_{1yy}}{\sigma_{D2yy} - \sigma_{D1yy}} = \frac{(\sigma_{2yy} - \sigma_{1yy}) \rho_0^2 \sigma_{2zz}}{1 - \sigma_{2zz}/\sigma_{1zz}}, \quad (3.17)$$

$$\begin{aligned} \frac{\delta\sigma_{zz}}{\delta\sigma_{Dzz}} &= \frac{\sigma_{2zz} - \sigma_{1zz}}{\sigma_{D2zz} - \sigma_{D1zz}} \\ &= \frac{(\sigma_{2zz} - \sigma_{1zz}) \rho_0^2 \sigma_{2yy}}{1 - \sigma_{2yy}/\sigma_{1yy}}, \end{aligned} \quad (3.18)$$

it is easy to see that the third of these ratios [Eq. (3.17)] can be made identical to the first two [Eqs. (3.15) and (3.16)] by changing the No. 1 constituent conductivity σ_{1zz} to

$$\sigma_{1zz}^* \equiv \frac{\sigma_{2yy} \sigma_{2zz}}{\sigma_{1yy}} \quad (3.19)$$

in the dual problem only, while the fourth ratio [Eq. (3.18)] can be made equal to the first two by changing σ_{1yy} to

$$\sigma_{1yy}^* \equiv \frac{\sigma_{2yy} \sigma_{2zz}}{\sigma_{1zz}} \quad (3.20)$$

in the dual problem only.

With these replacements, the dual problem now involves the dual conductivity tensors $\hat{\sigma}_{D1}^*$ and $\hat{\sigma}_{D2}$, where $\hat{\sigma}_1^*$, $\hat{\sigma}_{D1}^*$ are obtained from $\hat{\sigma}_1$, $\hat{\sigma}_{D1}$ by replacing σ_{1yy} , σ_{1zz} by σ_{1yy}^* , σ_{1zz}^* , respectively, e.g.,

$$\hat{\sigma}_1^* = \begin{pmatrix} \sigma_{1xx} & \sigma_{1xy} & 0 \\ \sigma_{1yx} & \sigma_{1yy}^* & 0 \\ 0 & 0 & \sigma_{1zz}^* \end{pmatrix}. \quad (3.21)$$

The two equations (3.5) and (3.6) are now proportional to each other, therefore the potential fields φ , φ_D are identical, when the same boundary conditions are in effect. It therefore follows, from Eqs. (3.7)–(3.14), that the ratios of the in-plane Ohmic components of $\hat{\sigma}_D^{(e)*} \equiv \hat{\sigma}_D^{(e)}(\hat{\sigma}_1^*, \hat{\sigma}_2)$ and $\hat{\sigma}^{(e)} \equiv \hat{\sigma}^{(e)}(\hat{\sigma}_1, \hat{\sigma}_2)$ are also equal to the rhs of Eqs. (3.15) and (3.16)

$$\frac{\sigma_{yy}^{(e)}}{\sigma_{Dyy}^{(e)*}} = \frac{\sigma_{zz}^{(e)}}{\sigma_{Dzz}^{(e)*}} = \frac{\sigma_{yz}^{(e)}}{\sigma_{Dyz}^{(e)*}} = \frac{\sigma_{zy}^{(e)}}{\sigma_{Dzy}^{(e)*}} = \rho_0^2 \sigma_{2yy} \sigma_{2zz}. \quad (3.22)$$

Using the explicit form of $\hat{\sigma}_D^{(e)}$ [Eq. (2.20)], we can rewrite these relations as

$$\begin{aligned} \sigma_{2yy} \sigma_{2zz} &= \frac{\sigma_{yy}^{(e)}}{\rho_{zz}^{(e)*} - \frac{\rho_{xz}^{(e)*} \rho_{zx}^{(e)*}}{\rho_{xx}^{(e)*}}} = \frac{\sigma_{zz}^{(e)}}{\rho_{yy}^{(e)*} - \frac{\rho_{xy}^{(e)*} \rho_{yx}^{(e)*}}{\rho_{xx}^{(e)*}}} \\ &= \frac{-\sigma_{yz}^{(e)}}{\rho_{zy}^{(e)*} - \frac{\rho_{xy}^{(e)*} \rho_{zx}^{(e)*}}{\rho_{xx}^{(e)*}}} = \frac{-\sigma_{zy}^{(e)}}{\rho_{yz}^{(e)*} - \frac{\rho_{xz}^{(e)*} \rho_{yx}^{(e)*}}{\rho_{xx}^{(e)*}}}. \end{aligned} \quad (3.23)$$

These exact relations between the bulk effective conductivities of the $\hat{\sigma}_1$, $\hat{\sigma}_2$ mixture and those of the $\hat{\sigma}_1^*$, $\hat{\sigma}_2$ mixture, where both mixtures have the same columnar microstructure but are otherwise arbitrary, are the main result of this paper. We note that the quantities which appear in Eq. (3.22) are all independent of σ_{ixx} , σ_{ixy} , σ_{iyx} , $i=1,2$. Thus, despite the appearance of xx , xy , yx , xz , and zx components of $\hat{\rho}^{(e)*}$ in Eqs. (3.23), those relations are also independent of σ_{ixx} , σ_{ixy} , σ_{iyx} , $i=1,2$. Therefore we could, for example, alter those components in $\hat{\sigma}_1^*$ of Eq. (3.21) without changing any of the results in Eqs. (3.22)–(3.24). We also note that $\hat{\sigma}_1^* = \hat{\sigma}_1$ whenever the following relation holds:

$$\sigma_{1yy} \sigma_{1zz} = \sigma_{2yy} \sigma_{2zz}. \quad (3.25)$$

In the special case of scalar conductivity tensors in both constituents $\hat{\sigma}_i = \sigma_i \hat{I}$, $i=1,2$, (this means that both constituents are isotropic conductors and that the magnetic field vanishes; \hat{I} is the unit tensor) Eqs. (3.19) and (3.20) reduce to $\sigma_1^* = \sigma_2^2 / \sigma_1$. In this case it is also clear that, due to the columnar nature of the microstructure, we must have $\rho_{xz}^{(e)} = \rho_{zx}^{(e)} = 0$. If y, z are the principal in-plane axes, then Eqs. (3.23) reduce to Keller's theorem, Eq. (1.1).

IV. APPLICATION TO CONDUCTOR/INSULATOR AND NORMAL CONDUCTOR/PERFECT CONDUCTOR MIXTURES

We assume that $\hat{\rho}_2$ represents a free-electron metal, i.e., that it has the form shown in Eq. (2.11), while $\hat{\sigma}_1 = 0$ represents a perfect insulator. We also assume that the metallic constituent percolates in the y, z plane, so that the entire system is a macroscopic conductor in all directions. In this case we have

$$\hat{\sigma}_1^* = \begin{pmatrix} 0 & 0 & 0 \\ 0 & \infty & 0 \\ 0 & 0 & \infty \end{pmatrix}. \quad (4.1)$$

However, the remarks which followed Eqs. (3.14) and (3.24) allow us to replace $\hat{\sigma}_1^*$ by the perfect conductor $\hat{\sigma}_1^{**} \equiv \infty \times \hat{I}$. We can now use results from Sec. II B: Eq. (2.17) leads to the normal conductor/perfect conductor mixture results

$$\begin{aligned} 0 &= \rho_{xx}^{(e)}(\hat{\rho}_1^{**}, \hat{\rho}_2) = \rho_{xy}^{(e)}(\hat{\rho}_1^{**}, \hat{\rho}_2) = \rho_{yx}^{(e)}(\hat{\rho}_1^{**}, \hat{\rho}_2) \\ &= \rho_{xz}^{(e)}(\hat{\rho}_1^{**}, \hat{\rho}_2) = \rho_{zx}^{(e)}(\hat{\rho}_1^{**}, \hat{\rho}_2), \end{aligned} \quad (4.2)$$

while Eq. (2.16) leads to the conductor/insulator mixture results

$$\begin{aligned} \rho_{xx}^{(e)}(\hat{\rho}_1, \hat{\rho}_2) &= \frac{\rho_0}{p_M}, \quad \rho_{yx}^{(e)}(\hat{\rho}_1, \hat{\rho}_2) = -\rho_{xy}^{(e)}(\hat{\rho}_1, \hat{\rho}_2) = \frac{\rho_0 H}{p_M}, \\ \rho_{xz}^{(e)}(\hat{\rho}_1, \hat{\rho}_2) &= \rho_{zx}^{(e)}(\hat{\rho}_1, \hat{\rho}_2) = 0. \end{aligned} \quad (4.3)$$

The exact relations of Eqs. (3.23) and (3.24) now become (note that $\sigma_{yz}^{(e)} = \sigma_{zy}^{(e)}$ and $\rho_{yz}^{(e)} = \rho_{zy}^{(e)}$)

$$\frac{\tilde{\sigma}_{\perp \text{ ins}}^{(e)}}{\rho_{\parallel \text{ sup}}^{(e)}} = \frac{\sigma_{\parallel \text{ ins}}^{(e)}}{\tilde{\rho}_{\perp \text{ sup}}^{(e)}} = -\frac{\sigma_{yz \text{ ins}}^{(e)}}{\rho_{yz \text{ sup}}^{(e)}} = \frac{1}{\rho_0^2 (1 + H^2)}. \quad (4.4)$$

Here the subscript ‘‘ins’’ refers to a conducting host with perfectly insulating inclusions, while the subscript ‘‘sup’’ refers to a conducting host with perfectly conducting inclusions, where both composites have the *same columnar microstructure*, with a volume fraction p_M of the (normal) conducting host constituent, but are otherwise arbitrary; the subscript \parallel and the tilde and subscript \perp refer to the zz and yy components of the tensor $\hat{\sigma}^{(e)}$, i.e., to the longitudinal and the in-plane transverse Ohmic (diagonal) components of the bulk effective conductivity tensor. We note that, in general, $\hat{\sigma}_{\text{ins}}^{(e)}$ and $\hat{\rho}_{\text{ins}}^{(e)}$, as well as $\hat{\sigma}_{\text{sup}}^{(e)}$ and $\hat{\rho}_{\text{sup}}^{(e)}$, will also have nonzero in-plane, off-diagonal, equal yz and zy components. Only when y and z lie along a sufficiently high-symmetry direction of the microstructure (i.e., a mirror symmetry plane) will those components vanish.²⁰ Also, in the case of a conductor/perfect insulator mixture, the xy and yx components of $\rho_{\text{ins}}^{(e)}$ are nonzero—see Eq. (4.3). For those reasons, one may not simply replace $\sigma_{\parallel}^{(e)}$ by $1/\rho_{\parallel}^{(e)}$, nor can one replace $\tilde{\sigma}_{\perp}^{(e)}$ by $1/\tilde{\rho}_{\perp}^{(e)}$. A similar sequence of considerations, invoked for the case where $\hat{\sigma}_1$ represents a perfect conductor, leads to

$$\frac{\tilde{\sigma}_{\perp \text{ sup}}^{(e)}}{\rho_{\parallel \text{ ins}}^{(e)}} = \frac{\sigma_{\parallel \text{ sup}}^{(e)}}{\tilde{\rho}_{\perp \text{ ins}}^{(e)} + \rho_0 H^2 / p_M} = - \frac{\sigma_{yz \text{ sup}}^{(e)}}{\rho_{yz \text{ ins}}^{(e)}} = \frac{1}{\rho_0^2 (1 + H^2)}. \quad (4.5)$$

Taking into account the off-diagonal elements of $\hat{\rho}_{\text{sup}}^{(e)}$ and $\hat{\rho}_{\text{ins}}^{(e)}$, in order to write Eqs. (4.4) and (4.5) entirely in terms of elements of those two tensors, we get, respectively,

$$\begin{aligned} \rho_0^2 (1 + H^2) &= \rho_{\parallel \text{ sup}}^{(e)} \left(\tilde{\rho}_{\perp \text{ ins}}^{(e)} + \frac{\rho_0 H^2}{p_M} - \frac{(\rho_{yz \text{ ins}}^{(e)})^2}{\rho_{\parallel \text{ ins}}^{(e)}} \right) \\ &= \tilde{\rho}_{\perp \text{ sup}}^{(e)} \left(\rho_{\parallel \text{ ins}}^{(e)} - \frac{(\rho_{yz \text{ ins}}^{(e)})^2}{\tilde{\rho}_{\perp \text{ ins}}^{(e)} + \rho_0 H^2 / p_M} \right) \\ &= \frac{\rho_{yz \text{ sup}}^{(e)}}{\rho_{yz \text{ ins}}^{(e)}} \left[\rho_{\parallel \text{ ins}}^{(e)} \left(\tilde{\rho}_{\perp \text{ ins}}^{(e)} + \frac{\rho_0 H^2}{p_M} \right) - (\rho_{yz \text{ ins}}^{(e)})^2 \right], \end{aligned} \quad (4.6)$$

$$\begin{aligned} \rho_0^2 (1 + H^2) &= \rho_{\parallel \text{ ins}}^{(e)} \left(\tilde{\rho}_{\perp \text{ sup}}^{(e)} - \frac{(\rho_{yz \text{ sup}}^{(e)})^2}{\rho_{\parallel \text{ sup}}^{(e)}} \right) \\ &= \left(\tilde{\rho}_{\perp \text{ ins}}^{(e)} + \frac{\rho_0 H^2}{p_M} \right) \left(\rho_{\parallel \text{ sup}}^{(e)} - \frac{(\rho_{yz \text{ sup}}^{(e)})^2}{\tilde{\rho}_{\perp \text{ sup}}^{(e)}} \right) \\ &= \frac{\rho_{yz \text{ ins}}^{(e)}}{\rho_{yz \text{ sup}}^{(e)}} (\tilde{\rho}_{\perp \text{ sup}}^{(e)} \rho_{\parallel \text{ sup}}^{(e)} - (\rho_{yz \text{ sup}}^{(e)})^2). \end{aligned} \quad (4.7)$$

After some simple algebraic manipulations, these equations can also be written in the following form:

$$\frac{\rho_{\parallel \text{ ins}}^{(e)}}{\rho_{\parallel \text{ sup}}^{(e)}} = \frac{\tilde{\rho}_{\perp \text{ ins}}^{(e)} + \frac{\rho_0 H^2}{p_M}}{\tilde{\rho}_{\perp \text{ sup}}^{(e)}} = \frac{\rho_{yz \text{ ins}}^{(e)}}{\rho_{yz \text{ sup}}^{(e)}} = \frac{\rho_{\parallel \text{ ins}}^{(e)} \left(\tilde{\rho}_{\perp \text{ ins}}^{(e)} + \frac{\rho_0 H^2}{p_M} \right) - (\rho_{yz \text{ ins}}^{(e)})^2}{\rho_0^2 (1 + H^2)} \quad (4.8)$$

$$= \frac{\rho_0^2 (1 + H^2)}{\rho_{\parallel \text{ sup}}^{(e)} \tilde{\rho}_{\perp \text{ sup}}^{(e)} - (\rho_{yz \text{ sup}}^{(e)})^2}, \quad (4.9)$$

where the result shown in the last line was derived from Eqs. (4.7), and the result in the line before that was derived from Eqs. (4.6).

These relations are in agreement with a similar one previously found to hold, empirically, for periodic composites in the strong field limit ($|H| \gg 1$), when \mathbf{B} points in some particular directions—cf. Eq. (4.1) in Ref. 15 with the second relation (i.e., the second line) of Eqs. (4.6) for the case where $\rho_{yz \text{ ins}}^{(e)}$ vanishes because $z \parallel \mathbf{B}$ lies along a mirror reflection plane of the microstructure. For $H = 0$, these relations reduce to $\rho_{\text{sup}}^{(e)} \rho_{\text{ins}}^{(e)} = \rho_0^2$, which can also be shown to follow from Keller's theorem, Eq. (1.1).

V. SOME TESTS AND CONSEQUENCES

The exact relations obtained in the previous section will now be tested on a number of theoretical and computational results which are currently available. These include results for ordered as well as for disordered columnar composites.

A. The columnar unambiguous effective medium approximation (CUSEMA)

The above mentioned approximation was recently developed for a disordered (percolating) system with columnar disorder and an in-plane magnetic field.¹⁴ That theory incorporates the exact results Eqs. (2.16) and (2.17). In the case of a conductor/insulator mixture, it was found that both the longitudinal and the in-plane transverse magnetoresistivities, $\rho_{\parallel \text{ ins}}^{(e)}$ and $\tilde{\rho}_{\perp \text{ ins}}^{(e)}$, are given by the same expression [see Eq. (4.8) in Ref. 14]

$$\begin{aligned} \frac{\tilde{\rho}_{\perp \text{ ins}}^{(e)}}{\rho_0} &= \frac{\rho_{\parallel \text{ ins}}^{(e)}}{\rho_0} \\ &= \frac{1}{\Delta p} \left[p_M + \frac{p_I^2 H^2}{2p_M} + p_I \left(1 + H^2 + \frac{p_I^2 H^4}{4p_M^2} \right)^{1/2} \right], \end{aligned} \quad (5.1)$$

where p_I and p_M are the volume fractions of the insulating and metallic constituents, and $\Delta p = p_M - p_I$. In the case of a normal conductor/perfect conductor mixture, $\rho_{\parallel \text{ sup}}^{(e)}$ and $\tilde{\rho}_{\perp \text{ sup}}^{(e)}$ are given by two different expressions [see Eqs. (4.18) and (4.19) in Ref. 14]

$$\frac{\tilde{\rho}_{\perp \text{ sup}}^{(e)} / \rho_0}{1 + H^2} = p_M + \frac{p_S^2 H^2}{2p_M} - p_S \left(1 + H^2 + \frac{p_S^2 H^4}{4p_M^2} \right)^{1/2}, \quad (5.2)$$

$$\frac{\rho_0}{\rho_{\parallel \text{ sup}}^{(e)}} = \frac{\rho_0}{\tilde{\rho}_{\perp \text{ sup}}^{(e)}} + \frac{H^2 / p_M}{1 + H^2}, \quad (5.3)$$

where p_S is the volume fraction of the perfectly conducting constituent. Because the system is now isotropic in the y, z plane, the yz component of $\hat{\rho}^{(e)}$ vanishes, and Eqs. (4.6)–(4.9) simplify appropriately. It is easily checked that the above results satisfy those simplified exact relations when we set $p_S = p_I = 1 - p_M$.

B. Periodic composite: numerical results

In recent years, studies have been published of the magnetotransport in columnar composites with a periodic microstructure, especially when the magnetic field is strong (i.e., $|H| \geq 1$) and perpendicular to the columnar axis. Those studies, which included numerical computations as well as experiments, revealed a striking dependence of the bulk effective, in-plane Ohmic resistivities and conductivities (i.e., the diagonal elements $\rho_{zz}^{(e)} \equiv \rho_{\parallel}^{(e)}$ and $\rho_{yy}^{(e)} \equiv \tilde{\rho}_{\perp}^{(e)}$ of the bulk effective resistivity tensor $\hat{\rho}_e$, and the similar elements $\sigma_{zz}^{(e)} \equiv \sigma_{\parallel}^{(e)}$ and $\sigma_{yy}^{(e)} \equiv \tilde{\sigma}_{\perp}^{(e)}$ of the bulk effective conductivity tensor $\hat{\sigma}_e$) on the precise in-plane directions of \mathbf{B} and $\langle \mathbf{J} \rangle$.^{20–22} In marked contrast with this behavior, Eqs. (3.22)–(3.24)

and (4.4)–(4.7) predict that certain combinations of these strongly oscillating resistivities or conductivities should be *independent of those directions*. Thus, numerical evaluations of those resistivities and conductivities can provide a highly nontrivial test of these equations. We now describe some tests of this kind. To that end, the bulk effective magnetoconductivity was calculated for various types of periodic composites detailed below, using the numerical approach described in Refs. 21, 23, and 24.

In order to test the predictions of Eqs. (4.4)–(4.9), we computed $\hat{\sigma}_{\text{ins}}^{(e)}$ and $\hat{\sigma}_{\text{sup}}^{(e)}$ for various values of H , assuming a free-electron-metal host. Actually, $\hat{\sigma}_{\text{sup}}^{(e)}$ was calculated using free-electron-metal inclusions with the large but finite zero-field conductivity $\sigma_1 = 100/\rho_0$. From those we then computed $\hat{\rho}_{\text{ins}}^{(e)}$ and $\hat{\rho}_{\text{sup}}^{(e)}$. In Figs. 2 and 3 we show polar plots of longitudinal and in-plane transverse Ohmic (diagonal) components of $\hat{\rho}_{\text{ins}}^{(e)}$ and $\hat{\rho}_{\text{sup}}^{(e)}$, along with some particular products or combinations, plotted vs the direction of \mathbf{B} . From Eqs. (4.4)–(4.7) it is predicted that those combinations will all appear as circles in such plots, with a definite magnetic-field-dependent radius, even though each resistivity component separately exhibits strong oscillations as function of the in-plane direction of \mathbf{B} .

The deviations from the precisely predicted circular plots in the right-hand parts of Figs. 2 and 3 can be ascribed to imperfect convergence of the numerical computations, and to the fact that the “perfectly conducting inclusions” were only 100 times more conducting than the normal conductor host. When the number of harmonics retained in the Fourier-based numerical scheme is increased, those deviations become smaller (see Refs. 21 and 23 for a detailed description of this numerical scheme). The deviations provide a good measure for the accuracy of the numerical computations.

C. Periodic composite: asymptotic expressions and phase-transition-like behavior

Very recently, it was discovered that closed-form expressions can sometimes be found for the asymptotic strong field ($|H| \gg 1$) values of the bulk effective, in-plane Ohmic magnetoconductivity components of columnar composites where a 2D periodic array of columnar inclusions are embedded in an otherwise uniform conducting host, when the inclusions are either perfect insulators or perfect conductors. This is possible when \mathbf{B} lies along sufficiently low order symmetry axes of the 2D array.^{15,16} It was also found that, in such directions, there appears a drastic, phase-transition-like change of macroscopic response, as well as of the local distribution of $\mathbf{E}(\mathbf{r})$ and $\mathbf{J}(\mathbf{r})$, when the inclusion size passes through a sharp threshold value.^{15,19}

It is easy to check that, in all cases where the relevant closed form asymptotic expressions were calculated in Ref. 15, Eqs. (4.4)–(4.9) are satisfied. In two cases, where exact asymptotic expressions were found for $\tilde{\rho}_{\perp \text{ins}}^{(e)}$, [see Eqs. (3.13) and (3.15) of that reference] but none were found for $\rho_{\parallel \text{sup}}^{(e)}$ in the same microstructures, we can use the first relation of Eqs. (4.6) or the second relation of Eqs. (4.7) to provide asymptotic expressions for the latter quantity too (note that $\rho_{yz}^{(e)} = \rho_{zy}^{(e)} = 0$ in those cases, because \mathbf{B} lies along the (011) direction, which is a mirror plane of the square-

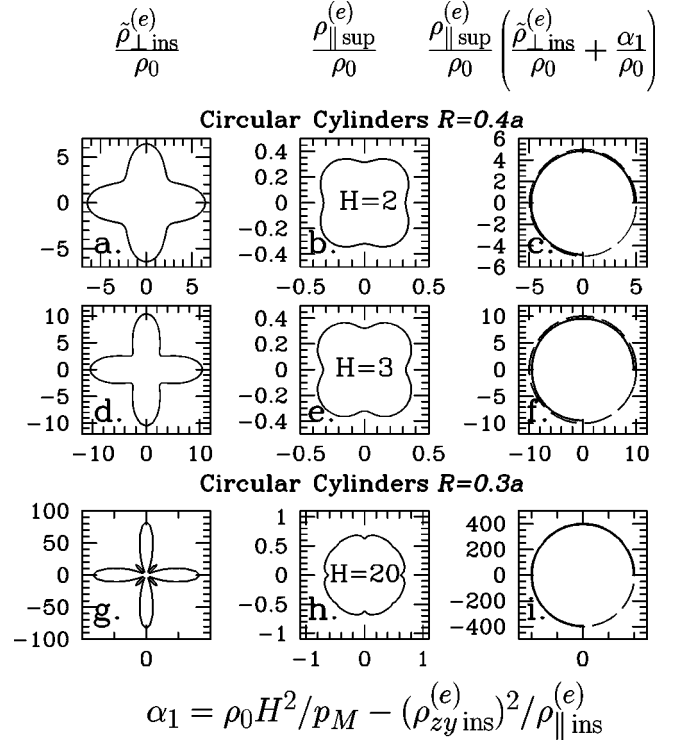


FIG. 2. Polar plots of $\tilde{\rho}_{\perp \text{ins}}^{(e)}/\rho_0$, $\rho_{\parallel \text{sup}}^{(e)}/\rho_0$, and of the combination $\rho_{\parallel \text{sup}}^{(e)}[\tilde{\rho}_{\perp \text{ins}}^{(e)} + \rho_0 H^2/p_M - (\rho_{yz \text{ins}}^{(e)})^2/\rho_{\parallel \text{ins}}^{(e)}]/\rho_0^2$, plotted vs the direction of \mathbf{B} . The left and middle columns represent numerical calculations on square arrays of infinitely long, parallel, circular cylinders, with radius R and unit-cell size a , embedded in an otherwise uniform, free-electron-like host with zero-magnetic-field conductivity $1/\rho_0 = 1$ and different values of the Hall-to-Ohmic resistivity ratio H , as shown in the three rows of plots. The cylindrical inclusions were either perfect insulators (i.e., with a vanishing scalar Ohmic conductivity; results shown in the left column), or “perfect conductors” (i.e., with a scalar Ohmic conductivity that is 100 times greater than that of the free-electron-like host; results shown in the middle column). Two different values were used for the ratio R/a , as shown in the figure. The combination which is plotted in the right-hand column should always be equal to $1 + H^2$ [see the first relation of Eqs. (4.6)] whatever the direction of \mathbf{B} —those circles are shown as dashed lines. The actual values of the products, as obtained from the numerical results, are shown as boldface lines in the same plots. The lower right-hand quadrant of the boldface line has been left out of these plots in order to facilitate visual identification of the dashed line circles.

symmetry microstructure). Similarly, the exact asymptotic expression found in one case for $\rho_{\parallel \text{ins}}^{(e)}$ [Eq. (3.39) of Ref. 15] can be combined with the second relation of Eqs. (4.6) or the first relation of Eqs. (4.7) to provide an asymptotic expression for $\tilde{\rho}_{\perp \text{sup}}^{(e)}$ in the same microstructure.

Equations (4.4)–(4.9) also provide important connections between some generic asymptotic behaviors found in Ref. 15. Thus, the fact that $\rho_{\parallel \text{sup}}^{(e)}$ always saturates but is nonisotropic when $|H| \gg 1$, whatever the direction of \mathbf{B} , can now be directly related to the fact that $\tilde{\rho}_{\perp \text{ins}}^{(e)} \propto H^2$ in that limit, whatever the direction of \mathbf{B} . Similarly, the fact that $\rho_{\parallel \text{ins}}^{(e)}$ saturates only when \mathbf{B} points along one of a small number of low order lattice axes can be directly related to the fact that $\tilde{\rho}_{\perp \text{sup}}^{(e)}$

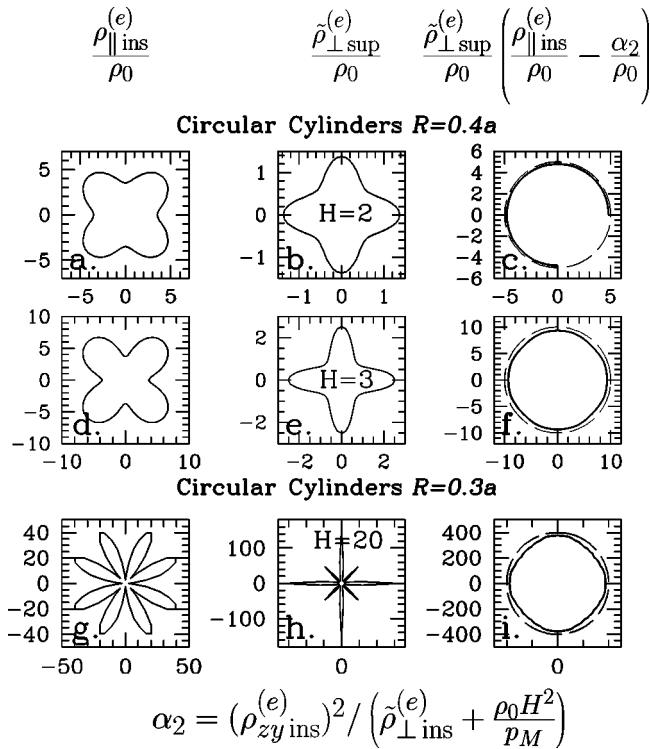


FIG. 3. Polar plots of $\rho_{\parallel \text{ins}}^{(e)}/\rho_0$, $\tilde{\rho}_{\perp \text{sup}}^{(e)}/\rho_0$, and of the combination $\tilde{\rho}_{\perp \text{sup}}^{(e)}[\rho_{\parallel \text{ins}}^{(e)} - (\rho_{yz \text{ins}}^{(e)})^2/(\tilde{\rho}_{\perp \text{ins}}^{(e)} + \rho_0 H^2/p_M)]/\rho_0^2$, plotted vs the direction of \mathbf{B} . The microstructure and physical parameters are the same as in Fig. 2. The left and middle columns show results of numerical computations for composites with the same microstructure, where the inclusions are perfectly insulating and perfectly conducting, respectively. Again, the combination plotted in the right-hand column should always be equal to $1 + H^2$ [see the second relation of Eqs. (4.6)] whatever the direction of \mathbf{B} —those circles are shown as dashed lines, while the actual values of the products, as obtained from the numerical results, are again shown as boldface lines on the same plots, with the lower right-hand quadrant sometimes omitted in the interests of clarity.

fails to saturate, increasing as H^2 , only when \mathbf{B} lies along those same axes.

Finally, $\rho_{\parallel \text{ins}}^{(e)}$ was shown to exhibit critical behavior when \mathbf{B} lies along any low order lattice axis, and the inclusion size

approaches a threshold value, where the inclusion-free slabs parallel to \mathbf{B} shrink to zero.¹⁹ This includes a drastic change from saturating behavior below the threshold to nonsaturating, $\rho_{\parallel \text{ins}}^{(e)} \propto H^2$ behavior above it, as well as a scaling dependence on two characteristic lengths, both of which tend to 0 at the threshold. Precisely at the threshold, $\rho_{\parallel \text{ins}}^{(e)} \propto |H|$ for $|H| \gg 1$. Using Eqs. (4.6) or (4.7), we can now make similar predictions for the critical behavior of $\tilde{\rho}_{\perp \text{sup}}^{(e)}$ in the same microstructure. These predictions, as well as those of Ref. 19, await experimental verification.

VI. SUMMARY

Keller's theorem [Eq. (1.1)], vis-a-vis bulk effective conductivity of a 2D, two-constituent composite medium, has been extended so as to apply to composites with a 3D columnar microstructure [Eqs. (3.23) and (3.24)]. This is particularly relevant for the case where both constituents are isotropic conductors and an external, in-plane magnetic field is applied, i.e., one that is perpendicular to the columnar axis. The theorem was applied to some special cases, including a conductor/insulator mixture and a normal conductor/perfect conductor mixture with the *same microstructure*. Exact, simple connections were thus found between the in-plane magnetoresistivities of such pairs of systems. Those relations were tested on some currently available theoretical and numerical results for columnar composites. An experimental verification of those relations would also be desirable. Applicability of the extended theorem is not restricted to columnar systems of infinite thickness. Finite thickness films will also satisfy it very well if the film thickness l , and the heterogeneity length scale a , and the Hall-to-Ohmic resistivity ratio of the normal conductor constituent H , satisfy the inequality $Hl \gg a$.

ACKNOWLEDGMENTS

This research was supported in part by grants from the U.S.-Israel Binational Science Foundation, the Israel Science Foundation, the Tel Aviv University Research Authority, and the Ministry of Absorption of the State of Israel.

¹R. Juretschke, R. Landauer, and J.A. Swanson, J. Appl. Phys. **27**, 838 (1956).
²J.B. Keller, J. Math. Phys. **5**, 548 (1964).
³A.M. Dykhne, Zh. Éksp. Teor. Fiz. **59**, 110 (1970) [Sov. Phys. JETP **32**, 63 (1971)].
⁴K.S. Mendelson, J. Appl. Phys. **46**, 917 (1975).
⁵K.S. Mendelson, J. Appl. Phys. **46**, 4740 (1975).
⁶K. Schulgasser, J. Math. Phys. **17**, 378 (1975).
⁷B.I. Shklovskii, Zh. Éksp. Teor. Fiz. **72**, 288 (1977) [Sov. Phys. JETP **45**, 152 (1977)].
⁸D. Stroud and D.J. Bergman, Phys. Rev. B **30**, 447 (1984).
⁹G.W. Milton, Phys. Rev. B **38**, 11 296 (1988).
¹⁰H. Christiansson, Phys. Rev. B **56**, 572 (1997).
¹¹A.M. Dykhne and I.M. Ruzin, Phys. Rev. B **50**, 2369 (1994).

¹²I. Ruzin and S. Feng, Phys. Rev. Lett. **74**, 154 (1995).
¹³O. Levy and R.V. Kohn, J. Stat. Phys. **90**, 159 (1998).
¹⁴D.J. Bergman and Y.M. Strelniker, Phys. Rev. B **60**, 13 016 (1999).
¹⁵D.J. Bergman and Y.M. Strelniker, Phys. Rev. B **59**, 2180 (1999).
¹⁶D.J. Bergman and Y.M. Strelniker, Phys. Rev. Lett. **80**, 3356 (1998).
¹⁷D.J. Bergman and Y.M. Strelniker, Superlattices Microstruct. **23**, 547 (1998).
¹⁸D.J. Bergman and Y.M. Strelniker, Phys. Rev. B **51**, 13 845 (1995).
¹⁹D.J. Bergman and Y.M. Strelniker, Europhys. Lett. **45**, 605 (1999).
²⁰M. Tornow, D. Weiss, K.v. Klitzing, K. Eberl, D.J. Bergman, and

- Y.M. Strelniker, Phys. Rev. Lett. **77**, 147 (1996).
- ²¹D.J. Bergman and Y.M. Strelniker, Phys. Rev. B **49**, 16 256 (1994).
- ²²K.D. Fisher and D. Stroud, Phys. Rev. B **56**, 14 366 (1998).
- ²³Y.M. Strelniker and D.J. Bergman, Phys. Rev. B **50**, 14 001 (1994).
- ²⁴Y.M. Strelniker and D.J. Bergman, Phys. Rev. B **53**, 11 051 (1996).